COMPOSITIONAL STRUCTURE OF THE LOWER LUNAR CRUST: INITIAL CONSTRAINTS FROM BASIN MINERALOGY C. M. Pieters[1*], P. J. Isaacson[1], L. A. Taylor[2], J. W. Head[1], D. Dhingra[1], R. Klima[3], N. Petro[4], D. Moriarty[1], R. Green[5], and J. Boardman[6] [1]Dept. Geological Sciences, Brown Univ., Providence, RI 02912, [2]Planetary Geosciences Inst., Univ. of Tenn., [3]JHU/APL, [4]NASA GSFC, [5]JPL, [6]AIG *(Carle_Pieters@brown.edu)

Introduction: With the return of the first lunar samples, several paradigm shifts occurred and now form the basis of our understanding of other terrestrial planets. The concept of a lunar magma ocean and development of a primary crust was recognized with the first samples [1]. The Moon was and has remained the type-example for magma ocean characterization. Furthermore, this differentiation event occurred in the earliest recorded time-frame for planetary evolution and was hypothesized to be global in nature. Magma ocean products and subsequent evolution are thus reflected in the compositional stratigraphy of the lunar crust. Apollo samples were collected from a restricted area on the lunar nearside and early remote sensing has shown that these samples are not fully representative of lunar crustal materials [e.g., 2, 3, 4]. However, modern instruments designed to directly measure and map mineralogy can be used to address global issues of these formative first billion years of terrestrial planet evolution. Discussed here are results from the Moon Mineralogy Mapper (M^3) on Chandrayaan-1 [5, 6, 7]. An important property of the M^3 design is that it provides mineral information derived from high spectral resolution NIR data in a high spatial resolution geologic context.

Using basin-scale impacts as probes to the interior, we evaluate the mineral composition of materials exposed at carefully selected basin-related features. Although basin structure is model-dependent [e.g. 8], we currently focus on the inner-most ring of basins which are thought to represent wholesale translation and uplift of deep-seated materials [e.g., 9]. We also examine basin impact melt products to the extent possible. Crustal-thickness estimates [e.g., 10] provide important first-order constraints on total thickness variations and possible depths tapped by specific basins.

M^3 Data. Shown in Fig. 1 are low resolution mosaics prepared from M^3 data. The locations of initial basins studied are labeled. The 1000 nm integrated band depth (IBD) readily distinguishes mafic-rich (high IBD) and feldspathic mafic-poor (low IBD) regions. Example M^3 spectra that illustrate the diversity of mineralogy that are derived from depth are shown in Fig. 2.

The first basin studied, Orientale, was shown to exhibit massive anorthosite across the entire Inner Rook Mountains (IRM) [11, 12]. The widespread presence of pure anorthosite was independently identified at basin rings and central peaks by Kaguya sensors [13]. At Orientale, no significant mafic lithologies were observed in the IRM, although noritic components were observed elsewhere in Orientale rings and deposits [12, 14, 15].

The Moscoviense basin appears to have excavated deeper into the crust [10]. Extensive feldspathic material is observed here, but embedded within it are several old, but compositionally distinct, geographically separated regions a few km in dimension that are highly mafic in character [16]. These include a low-Ca orthopyroxene lithology, an olivine-rich lithology, and a new Mg-spinel dominated lithology (without detectible pyroxene or olivine), together called OOS. The presence of the new Mg-spinel lithology deep in the lower crust has been confirmed by the identification of similar materials in the central peaks of the crater Theophilus, which has excavated materials from the inner ring of Nectaris basin [17]. One of the M^3 olivine-rich OOS areas at Moscoviense is also part of a family of local olivine-rich regions detected by the Kaguya spectral profiler associated with several basins [18].

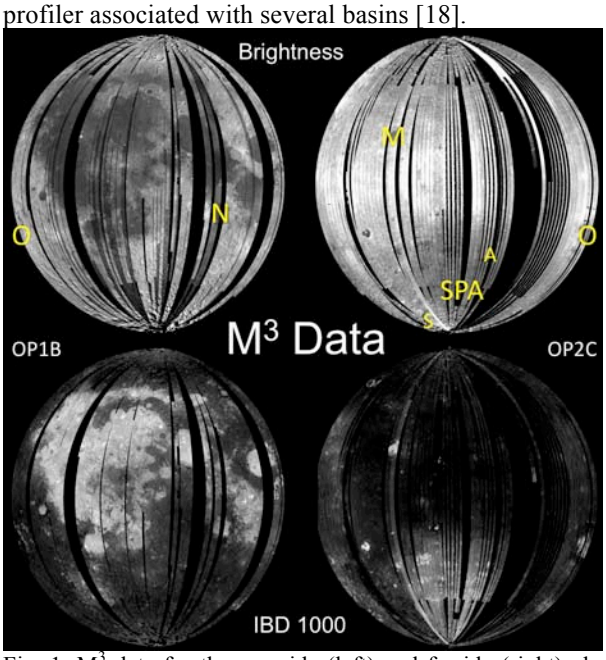

Fig. 1. M^3 data for the nearside (left) and farside (right) obtained during optical periods 1 and 2 respectively. Integrated band depth (IBD) is a good measure of mafic mineral relative abundance. Basins under study include Orientale (O), Moscoviense (M), South Pole-Aitken (SPA), Nectaris (N), Apollo (A), and Schrödinger (S).

The basin that is expected to have excavated deepest into the crust/mantle is the largest and oldest, South Pole-Aitken Basin (SPA) [19]. Unlike some of the younger basins, no equivalent of an inner peak ring has been confidently identified. In contrast to many of the

major basins on the lunar nearside, the central portion of the basin has not been covered by mare basalts, and SPA retains a mafic-rich signature across the basin that is presumed to be ancient [3]. We assume that much of this non-mare mafic anomaly represents products of the basin-forming event, and as such contains a mixture of the crustal column that was reprocessed as impact melt and/or breccia. As noted from Clementine data [20], most of the SPA non-mare material is noritic in composition (contains low-Ca pyroxene), but the pre-Nectarian center of the basin exhibits a different mafic lithology. Both M^3 and Kaguya SP show that highly noritic compositions are observed at several SPA central peak craters [21, 22]. M^3 data also show that the non-mare mineralogy of the central region centered on "Mafic Mound" contains more Fe- and Ca-rich mafic minerals than elsewhere in the basin.

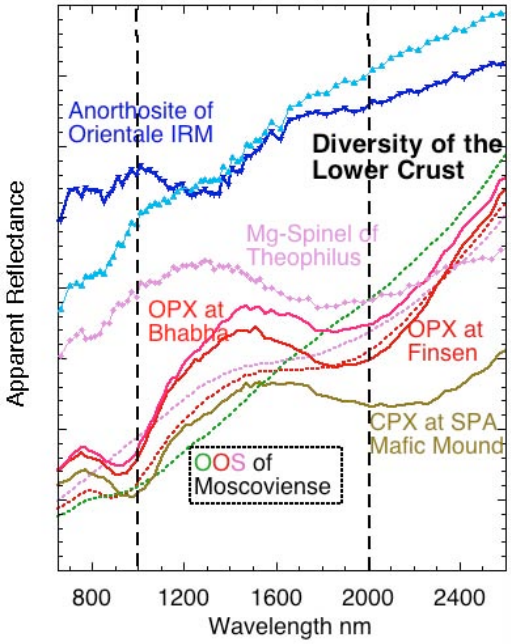

Fig. 2. M^3 Apparent Reflectance of basin ring materials and hypothesized basin impact melt. Deep-seated lithologies exposed include Anorthosite across Orientale IRM, Mg-spinel at Theophilus (Nectaris), Low-Ca pyroxene at the central peaks of SPA Bhabha and Finsen, Fe-and Ca-rich pyroxene at SPA Mafic Mound, and Orthopyroxene, Olivine, and Mg-Spinel (OOS) at Moscoviense. The OOS are well developed soils and have relatively steep continua [16]. The reflectance scale for Orientale and Theophilus spectra is twice that of the other spectra. Vertical lines are provided at 1000 and 2000 nm for ease of comparison.

Crustal Model. Although specific details of global mineralogy are currently incomplete, a schematic model of crustal stratigraphy depicted in Fig. 3 is consistent with the above mineralogical observations at basins that have been observed to date:

1. The megaregolith is dominated by processed noritic anorthosite breccias.
2. Lunar highland rocks are not all breccias. Outcrops of distinctive lithologies occur on scales of 10s of m to kms [16, 17].
3. Massive (ferroan) anorthosite occurs below the megaregolith as predicted by the magma ocean model.
4. The lower crust contains diverse lithogies, often highly mafic and Mg-rich (orthopyroxene, olivine, Mg-spinel). These appear to be embeded in an anorthositic matrix.
5. The deepest crust, perhaps upper mantle, contains more Fe- and Ca-rich lithologies (High-Ca pyroxene, olivine).

This mineralogical model of crustal structure leaves several issues open: What it the origin and scale of the Mg- and Fe-rich zones (layered intrusions, mantle overturn products, etc.)? What is their relation to the mantle? What is the role of KREEP and other heat sources?

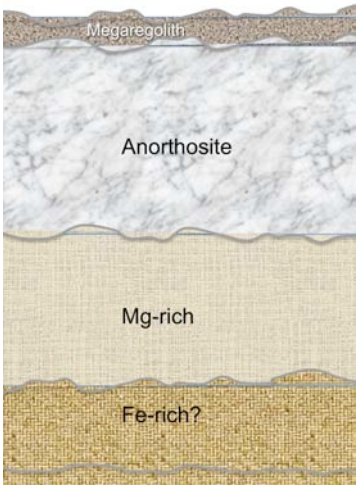

Fig. 3. Schematic cross-section of the compositional structure of the lunar crust based on mineral lithologies that have been observed along the innermost basin rings and as presumed impact melt products. Vertical scale varies with local geology and requires geophysical modeling with modern data. (The presence or absence of KREEP-rich materials is not addressed here.)

References: [1] Wood et al. (1970) *Proc. Apollo 11 Sci. Conf*., 965. [2] Pieters (1978) *PLSC9th*, 2825. [3] Jolliff et al., (2000) *JGR*, 105, E2, 4197. [4] Prettyman et al. (2006) *JGR*, 111, E12007. [5] Pieters CM et al. (2009) *Curr. Sci,* Vol. 96, No. 4, 500. [6] Green, RO et al. (2011) *JGR* submitted; and these volumes. [7] Boardman J et al. (2011) *JGR*, in press; and these volumes. [8] Melosh HJ (1989) *Impact cratering: A geologic process*. [9] Head JW (2010) *GRL*, 37, L02203. [10] Ishihara et al. (2009) *GRL*, 36, L19202. [11] Hawke et al. (1991) *GRL*, 18, 2141. [12] Pieters et al. (2009), *LPSC40* #2052. [13] Ohtake et al., (2009) *Nature* 461, 236. [14] Head et al., (2010) LPSC41 #1030. [15] Whitten et al. (2011) *JGR* in press and these volumes. [16] Pieters et al. (2010) LPSC41 #1854 and JGR in press. [17] Dhingra et al. (2011) these volumes. [18] Yamamato et al (2010) *Nature Geoscience*, Vol 3, 533. [19] Wilhelms DE (1987) *Geologic History of the Moon.* [20] Pieters et al. (2001) *JGR*, 106, E11, 28001. [21] Nakamura et al. (2009) *GRL*, 36, L22202. [22] Moriarty et al. (2011) these volumes.